Brain Tumor Semantic Segmentation using Residual U-Net++ Encoder-Decoder Architecture

Mai Mokhtar[1], Hala Abdel-Galil[2], Ghada Khoriba[3]

Computer Science Department-Faculty of Computers and Artificial Intelligence, Helwan University, Cairo, Egypt[1,2,3]
School of Information Technology and Computer Science ITCS, Nile University, Giza, Egypt [3]

***Abstract*—Image segmentation is considered one of the essential tasks for extracting useful information from an image. Given the brain tumor and its consumption of medical resources, the development of a deep learning method for MRI to segment the brain tumor of patients' MRI is illustrated here. Brain tumor segmentation technique is crucial in detecting and treating MRI brain tumors. Furthermore, it assists physicians in locating and measuring tumors and developing treatment and rehabilitation programs. The residual U-Net++ encoder-decoder-based architecture is designed as the primary network, and it is an architecture that is hybridized between ResU-Net and U-Net++. The proposed Residual U-Net++ is applied to MRI brain images for the most recent and well-known global benchmark challenges: BraTS 2017, BraTS 2019, and BraTS 2021. The proposed approach is evaluated based on brain tumor MRI images. The results with the BraST 2021 dataset with a dice similarity coefficient (DSC) is 90.3%, sensitivity is 96%, specificity is 99%, and 95% Hausdorff distance (HD) is 9.9. With the BraST 2019 dataset, a DSC is 89.2%, sensitivity is 96%, specificity is 99%, and HD is 10.2. With the BraST 2017 dataset, a DSC is 87.6%, sensitivity is 94%, specificity is 99%, and HD is 11.2. Furthermore, Residual U-Net++ outperforms the standard brain tumor segmentation approaches. The experimental results indicated that the proposed method is promising and can provide better segmentation than the standard U-Net. The segmentation improvement could help radiologists increase their radiologist segmentation accuracy and save time by 3%.**

***Keywords*—Brain tumor segmentation; medical image segmentation; BraTS; U-Net; U-Net++; residual network**

I. Introduction

Brain tumors are growing in the cells of the human brain abnormally. They are divided into two main types, which are malignant and benign, and malignant is more widely spread than benign. They have a significant impact on people and society. Gliomas, either high-grade gliomas (HGG) or low-grade gliomas (LGG), comprise the majority of malignant brain tumors. Because it enables medical professionals to find and quantify tumors and develop strategies for their treatment and recovery, brain tumor segmentation is crucial for diagnosing and treating brain tumors. Medical image segmentation divides a medical image into different regions and separates anatomical structures. These are called "regions of interest" and are appropriate for a specific medical application [1], [2].

There are two main medical image segmentation techniques: manual and auto segmentation. Manual segmentation is the gold standard approach that still consumes time and effort, not only time and effort but also needs experts. Auto segmentation techniques are divided into many techniques: region-based, edge-based, thresholding, atlas-based, clustering, and deep learning.

It is used in clinical studies to guide and monitor disease progression. It also has many uses, such as diagnosing diseases, planning treatments, studying anatomy, finding the problem, figuring out how much tissue there is, and doing computer-integrated surgery.

According to all of these usages, medical image segmentation has many challenges. These challenges are noise, different colors, patterns, orientations, textures, and insufficient resolution. Furthermore, the medical image is heterogeneous in shape, volume, and texture. These challenges make the segmentation task more complex and require multiple preprocessing approaches.

Recently, it has been suggested that deep learning methods could be used to make different applications for segmenting and classifying medical images. Deep Learning networks can segment and pull out features so that segmentation can be done with just one prediction model [3].

The deep learning model for medical images is classified into two main categories: 2D Fully Convolution Networks, such as U-Net architecture, and 3D Fully Convolutional Networks, where 2D convolutions are covered with 3D convolution.

Image segmentation is one of several deep learning-based applications being researched in the medical field. Consequently, there are several techniques and numerous network architectures. Based on its attributes, such as network design, training procedure (supervised, semi-supervised, unsupervised, and transfer learning), and input size (patch-based, whole volume-based, 2D, and 3D), segmentation techniques based on deep learning may be subdivided into several categories according to network design, training procedure, and input size. Therefore, depending on its architecture, it may be split into six categories: convolutional neural networks, fully convolutional networks; regional convolutional networks; auto-encoders; generative adversarial networks; and hybrid deep learning-based approaches.

The proposed Residual U-Net++ pipeline with the whole phases is shown in Fig. 1 and illustrated step by step for each phase as an overview.

This paper's main contributions are summarized as follows:

- A new hybridization approach based on U-Net++ and

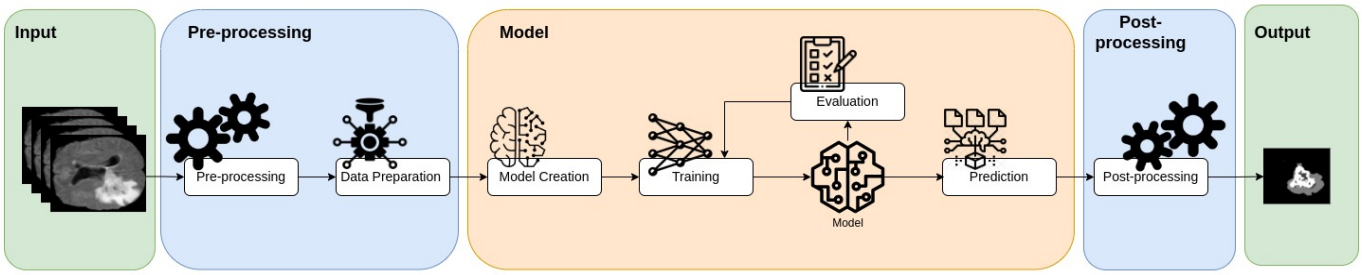

Fig. 1. Proposed residual U-Net++ pipeline.

ResU-Net is introduced, which combines the advantages of both architectures to improve the accuracy of brain tumor segmentation.

- A novel combination of pre-processing techniques and loss functions is proposed, further enhancing the hybrid approach's performance.
- The proposed Residual U-Net++ architecture is applied to three global benchmark challenges in brain tumor segmentation, including BraTS 2017, BraTS 2019, and BraTS 2021, and outperforms several state-of-the-art methods in all challenges, thus contributing significantly to the field.
- A discrete version of Residual U-Net++ is presented, specifically designed to address multi-level segmentation problems, and evaluated on a public benchmark real abdominal MRI images dataset of the brain as a case study.
- Several evaluation metrics, including the Dice Similarity Coefficient (DSC), Sensitivity (SEN), Specificity (SP), and 95% Hausdorff Distance (HD), are used to comprehensively assess the performance of the proposed approach, thus contributing to the standardization of evaluation methods in medical image segmentation research.

The rest of the paper is structured as follows: Section II represents the related work, Section III explains the details used in the model, which are dataset, pre-processing, architecture, loss function, and evaluation metrics. Section IV shows the results, followed by a discussion of the results in Section V. Finally, Section VI presents the conclusion.

II. Related Work

Zhang et al. [4] examine the significance of a newly created attention gate for tasks involving segmenting brain tumors as an attention module. They use datasets from BraTS, which are BraTS 2017, BraTS 2018, and BraTS 2019. They focus on investigating the efficacy of attention gates for tasks involving segmenting brain tumor images. They propose a model called the Attention Gate Residual U-Net, or AGResU-Net, which combines attention gates and residual modules within a fundamental and singular U-Net architecture to accomplish this purpose.

Neural Architecture Search (NAS) makes good progress in improving image accuracy. Accordingly, it has been extended to be used recently in image segmentation. Weng et al. [5] use NAS with U-Net as U-Net is applied a lot in different medical image segmentation with successful results. Therefore, both are used by Weng et al. [5] to design and develop three primitive operations that make search space that find two cell architectures, DownSC and UpSC, useful in medical image segmentation especially. Their dataset without pre-training was PASCAL VOC2012 which consisted of Magnetic Resonance Imaging (MRI), Computed Tomography (CT), and ultrasound. It gets better performance and fewer parameters than U-Net when evaluated on the three datasets [5].

Li et al. [6] proposed Residual-Attention U-Net++ as an extension of the U-Net++ model with a residual unit and attention mechanism. In angiography, they used three medical image datasets, skin cancer, cell nuclei, and coronary artery. Their results with the skin cancer dataset were an Intersection over Union (IoU) was 82.32% and a dice coefficient was 88.59%, and with the cell nuclei dataset, an IoU was 87.74%. The dice coefficient was 85.91%, and with the angiography dataset, an IoU was 66.57%, and a dice coefficient was 72.48%.

III. Materials and Method

A. Dataset

BraTS stands for Brain Tumor Segmentation, collected and prepared as a challenge per year. It is the most commonly used dataset for brain tumor segmentation as it is public [7], [8], [9], [10], [11], [12], [13], [14], [15]. It consists of a collection of MRI brain images, and all brain images are stripped of the skull and oriented similarly. Four MRI modalities exist for each patient, including Flair, T1, T1ce, and T2. The experts and the organizers of BraTS were labeling the training dataset ground truths. The example MRI brain image and associated ground truth are shown in Fig. 2.

On three benchmarks (BraTSraTS 2017, BraTS 2019, and BraTS 2021), we evaluate the effectiveness of ResU-Net++. Table I contains detailed information about the three datasets used for each year's challenge.

The BraTS 2017 dataset provides 285 glioma patients as a training dataset, consisting of 210 HGG cases and 75 LGG cases. There are 46 patients of uncertain grades included as validation dataset.

The BraTS 2019 dataset provides 335 glioma patients as a training dataset, consisting of 259 HGG cases and 76 LGG

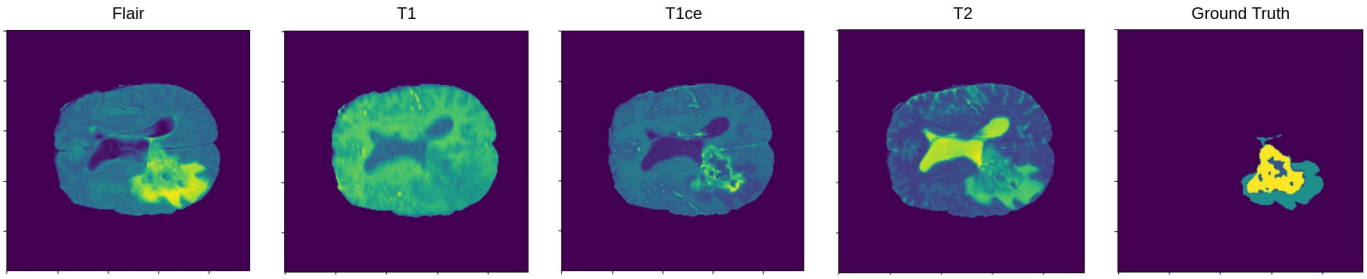

Fig. 2. Example of the brain MRI image with its ground truth from the BraTS 2019.

TABLE I. PUBLIC DATASETS THAT ARE USED FOR BRAIN TUMOR SEGMENTATION.

Name	Total Data Size	Training Data	Validation Data	Testing Data
BraTS 2017	477	285	46	146
BraTS 2019	653	335	127	191
BraTS 2021	2000	1251	219	530

cases. There are 127 patients of uncertain grades included as validation dataset.

The BraTS 2021 dataset provides 1251 glioma patients as a training dataset, which contains more patient cases than the previous two. There are 219 patients of uncertain grades included as validation dataset.

BraTS 2017 is used the most often because it is the first release to include training, validation, and test data. It is used in benchmarks and can be used with low computational power, in contrast to BraTS 2021. BraTS 2021 needs high computational power, takes more time, and gives high accuracy due to extensive data.

B. Proposed Residual U-Net++ Pre-processing

As discussed before, MRI brain tumor segmentation is a problem that is challenging due to noise, different colors, patterns, orientations, textures, and heterogeneous shapes, volumes, and textures. Data processing is still an essential and crucial stage, even if deep learning-based techniques are more noise-resistant. Furthermore, we use multimodal 3D MRI brain scan datasets, specifically BraTS 2017, BraTS 2019, and BraTS 2021, in this study. The normal region takes up 98.5% of the pixels in the multilabel brain tumor segmentation, whereas the abnormal area only makes up 1.5% of the pixels. Each 3D MRI image data set in the BraTS database has a volume size of 240 x 240 x 155. That image of the axial brain has the highest resolution, and the plane of the axial generates most of the volume in the dataset. We employ a 3D axial brain image to construct multiple 2D image slices for each 240 × 240. To create a sequence of 2D slice images, we remove the 3D image's 1% highest voxel intensities and 1% lowest voxel intensities. While this is happening, we use a patching technique to process these 2D image slices, cropping each slice into many tiny patches with a size of 128 × 128 to handle the class imbalance issue.

Furthermore, we use z-score normalization on 2D images. Moreover, Gaussian regularisation also on 2D images to limit the device noise effect, improve the contrast of an image, and relieve the overfitting problem. The Z-score normalization technique transforms each picture using the intensity's mean value and standard deviation, and it is calculated as follows:

$$z' = \frac{z - \mu}{\sigma} \tag{1}$$

Where z is the input image, z' is the normalized image, μ is the input image mean, and σ is the input image standard deviation.

In addition, Gaussian regularisation also involves adding Gauss noise to images to increase model training accuracy. It efficiently reduces over-fitting during the model training phase by penalizing interference objects produced by noise for lowering the weighted square, which has an equivalent impact as L2 regularisation. These images of 2D patches are used in the network for segmenting brain tumors as input after data pre-processing for balancing data voxels. This data preparation step could improve the segmentation performance, normalizing the data and successfully handling the class imbalance issue.

C. Proposed Residual U-Net++ Architecture

This paper introduced ResU-Net++, an integrated neural network for medical image segmentation that uses the benefits of U-Net++ and residual units. Its general layout is shown in Fig. 3. As we can see, the suggested architecture uses redesigned skip paths to connect the encoder and decoder networks, with U-Net++ as the primary network structure. The encoder network's feature map was sent to the decoder network through dense convolution blocks. According to the above-mentioned method, the feature graph semantic levels in the encoder and decoder are almost identical.

The skip pathway was constructed as follows: The node's output is represented by $x^{i,j}$. According to the encoder subnetwork, the downsampling layer is indexed by i, and the dense block's convolution layer is indexed by j along the skip

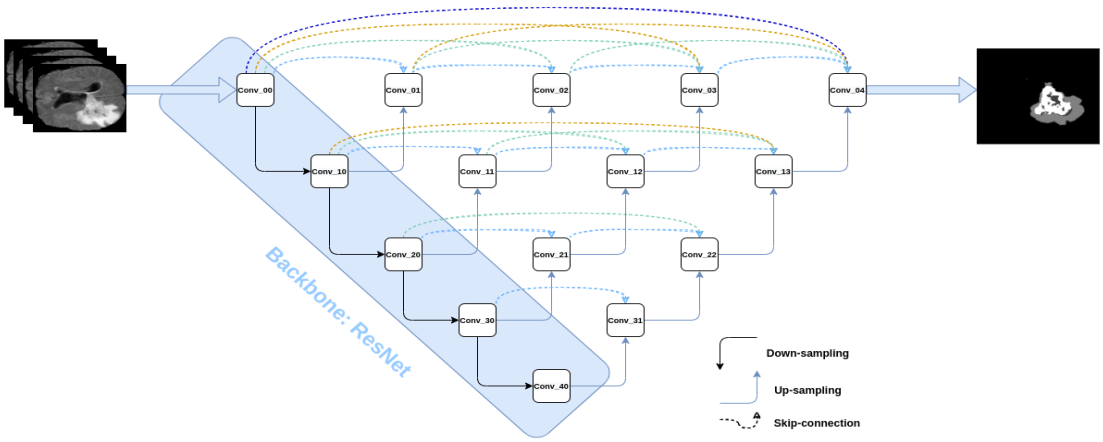

Fig. 3. Proposed residual U-Net++ architecture.

pathway. The mathematical equation that follows can be used to determine $x^{i,j}$:

$$x^{i,j} = \begin{cases} CR\{x^{i-1,j}\}, & j = 0. \\ CR\left\{\left[\int_{i-1}^{k=0} x^{i,k}, U(x^{i+1,j-1})\right]\right\}, & j > 0. \end{cases} \quad (2)$$

Where $[.]$ signifies the concatenation layer, $U(.)$ stands for the upsampling operations, and $CR\{.\}$ represents a convolution operation followed by a ReLU activation. The first skip pathway in Residual U-Net++ is further explained in Fig. 4.

The following applied equations illustrate the detailed analysis of the first skip pathway of Residual U-Net++:

$$x^{0,1}(conv\_01) = CR\{[x^{0,0}, U(x^{1,0})]\} \quad (3)$$

$$x^{0,2}(conv\_02) = CR\{[x^{0,0}, x^{0,1}, U(x^{1,1})]\} \quad (4)$$

$$x^{0,3}(conv\_03) = CR\{[x^{0,0}, x^{0,1}, x^{0,2}, U(x^{1,2})]\} \quad (5)$$

$$x^{0,4}(conv\_04) = CR\{[x^{0,0}, x^{0,1}, x^{0,2}, x^{0,3}, U(x^{1,3})]\} \quad (6)$$

This pairing has two advantages: first, U-Net++ reduces the semantic gap between the feature maps of the encoder and decoder subnetworks; second, the residual unit makes network training easier and solves the degradation issue, increasing the accuracy of Residual-Attention U-Net++.

D. Loss Function

The MRI brain tumor segmentation challenge displays a significant class imbalance, with healthy voxels making up 98.46% of the total voxels, necrosis and non-enhancing voxels accounting for 0.23% of voxels, edema accounting for 1.02% of voxels, and enhancing tumors accounting for 0.29% of voxels. Generalized dice loss (GDL) [16] is a loss function often used and resistant to data imbalance. It helps bridge the gap between evaluation metrics and training samples. Weighted cross entropy (WCE) [17] has also been used to solve class imbalance and multi-task training problems. As a result, we developed a union loss function L that combined generalized dice loss L_{GDL} and weighted cross entropy loss L_{WCE} to give improved supervision for model training [18]. Loss function L is represented as follows:

$$L = L_{GDL} + \lambda . L_{WCE} \quad (7)$$

where L_{GDL} represents the generalized dice loss is defined as Eq. 8 and L_{WCE} represents the weighted cross entropy loss is defined as Eq. 9

$$L_{GDL} = 1 - 2\frac{\sum_{i=1}^{N} \omega_i \sum_k g_{ik} p_{ik}}{\sum_{i=1}^{N} \omega_i \sum_k (g_{ik} + p_{ik})} \quad (8)$$

$$L_{WCE} = -\sum_k \sum_{i=1}^{N} \omega_i g_{ik} \log(p_{ik}) \quad (9)$$

Where N is the total number of labels, and ω_i is the weight for the ith label. For generalized dice loss, ω_i is set to

$$\omega_i = \frac{1}{(\sum_k g_{ik})} \quad (10)$$

p_{ik} represents the ith and kth pixel of the segmented binary image value.

g_{ik} represents the ith and kth pixel of the binary ground truth image value.

E. Evaluation Metrics

There are four evaluation metrics used in measuring segmentation performance for Residual U-Net++ approach. These metrics are examined by comparing the segmented image P to the manually segmented image T.

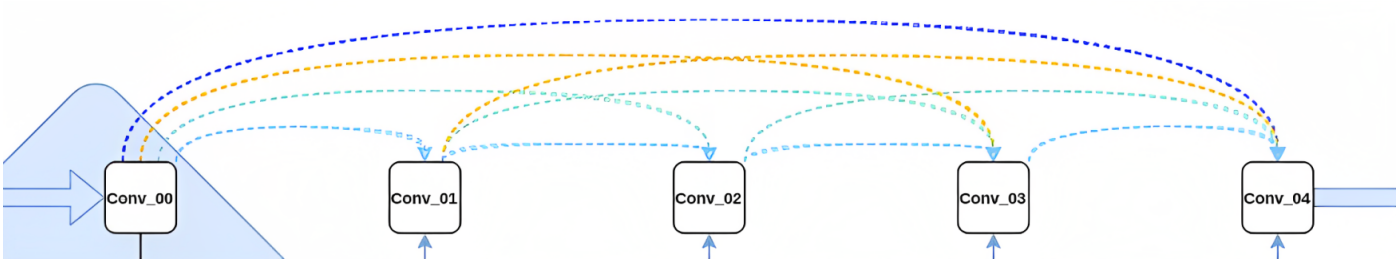

Fig. 4. The first skip pathway of residual U-Net++.

1) Dice Similarity Coefficient (DSC): The dice similarity coefficient is a metric to measure the performance of the segmentation that is used to evaluate it based on the intersection between both segmented images, manual and predicted, given as

$$DSC = 2\frac{|T \cap P|}{|T| + |P|} \tag{11}$$

Where T represents the manually segmented image as several elements, and P represents the predicted segmented image sets as several elements. Zero is the worst DSC value, and one is the best [19].

2) Sensitivity (SEN): Sensitivity is a metric to measure the performance of true positives of the correct detection ratio, given as

$$SEN = \frac{|TP|}{|TP| + |FN|}100 \tag{12}$$

Where TP is the number of correctly detected positive pixels (a "true positive"), FP is the number of incorrectly detected negative pixels (a "false positive"), and FN is the number of incorrectly detected positive pixels (a "false negative") [19].

3) Specificity (SP): Specificity is a metric to measure the performance of true negatives of the correct detection ratio, given as

$$SP = \frac{|TN|}{|TN| + |FP|}100 \tag{13}$$

Where TN is the number of correctly detected negative pixels (a "true negative"), and FP is the number of incorrectly detected negative pixels (a "false positive") [19].

4) Ninety-Five Percentage Hausdorff Distance (HD): Ninety-five percent Hausdorff distance is a performance metric that measures the 95^th percentile of the maximum distance of the reference image set to the nearest point in the predicted image set, given as

$$HD(P,T) = max[d(T,P), d(P,T)], \tag{14}$$

Where T represents the number of elements in the manually segmented image, and P represents the number of elements in the predicted segmented image sets. Both are a finite set [19].

Regarding all of these performance metrics that we used, each one of them is used according to need. DSC is the most accurate performance metric due to evaluating the intersection between manual and predicted segmented images, and it is the most commonly used. Also, HD is the second performance metric that is frequently used. SEN is used when the true positives are the attention point, and SP is used when the true negatives are the attention point.

IV. Results

As mentioned above, our experiments use three datasets: BraTS 2017, BraTS 2019, and BraTS 2021.

A. BraTS 2017

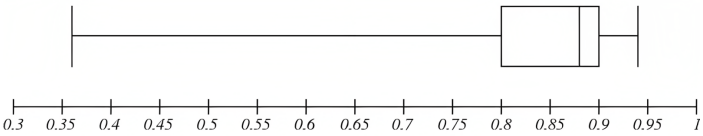

Fig. 5. Box plot for the DSC of results from the BraTS 2017 dataset.

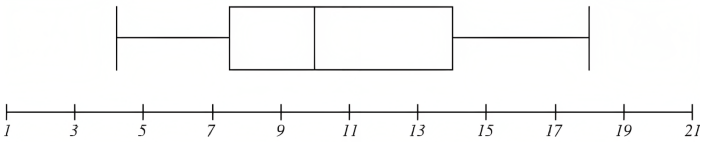

Fig. 6. Box plot for the HD of results from the BraTS 2017 dataset.

B. BraTS 2019

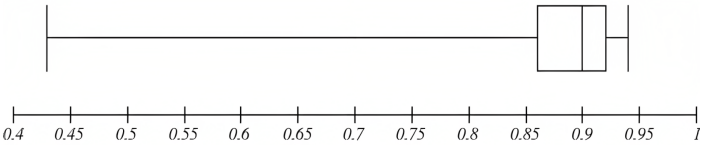

Fig. 7. Box plot for the DSC of results from the BraTS 2019 dataset.

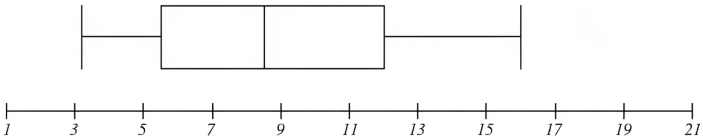

Fig. 8. Box plot for the HD of results from the BraTS 2019 dataset.

TABLE II. COMPARED SEGMENTATION RESULTS WITH DIFFERENT DSC METHODS FOR BRATS 2017

Author	Method	Whole	Core	Enhancing
Zhang et al. [4]	U-Net	0.852	0.759	0.698
Zhang et al. [4]	ResU-Net	0.862	0.774	0.732
Zhang et al. [4]	AGResU-Net	0.870	0.777	0.709
Proposed	**Residual U-Net++**	**0.876**	**0.862**	**0.833**

TABLE III. COMPARED SEGMENTATION RESULTS WITH DIFFERENT DSC METHODS FOR BRATS 2019

Author	Method	Whole	Core	Enhancing
Zhang et al. [4]	AGResU-Net	0.870	0.777	0.709
Aboelenein et al. [20]	MIRAU-Net	0.885	0.879	0.818
Sheng et al. [21]	ResU-Net	0.881	0.796	0.707
Proposed	**Residual U-Net++**	**0.892**	**0.892**	**0.853**

C. BraTS 2021

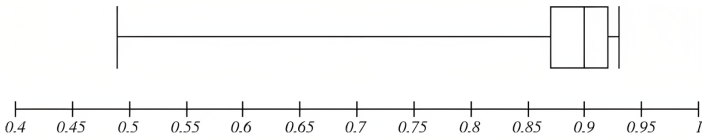

Fig. 9. Box plot for the DSC of results from the BraTS 2021 dataset.

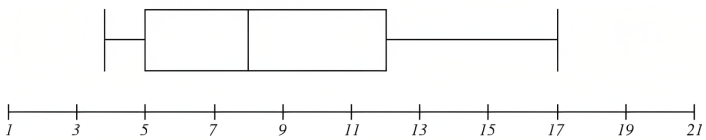

Fig. 10. Box plot for the HD of results from the BraTS 2021 dataset.

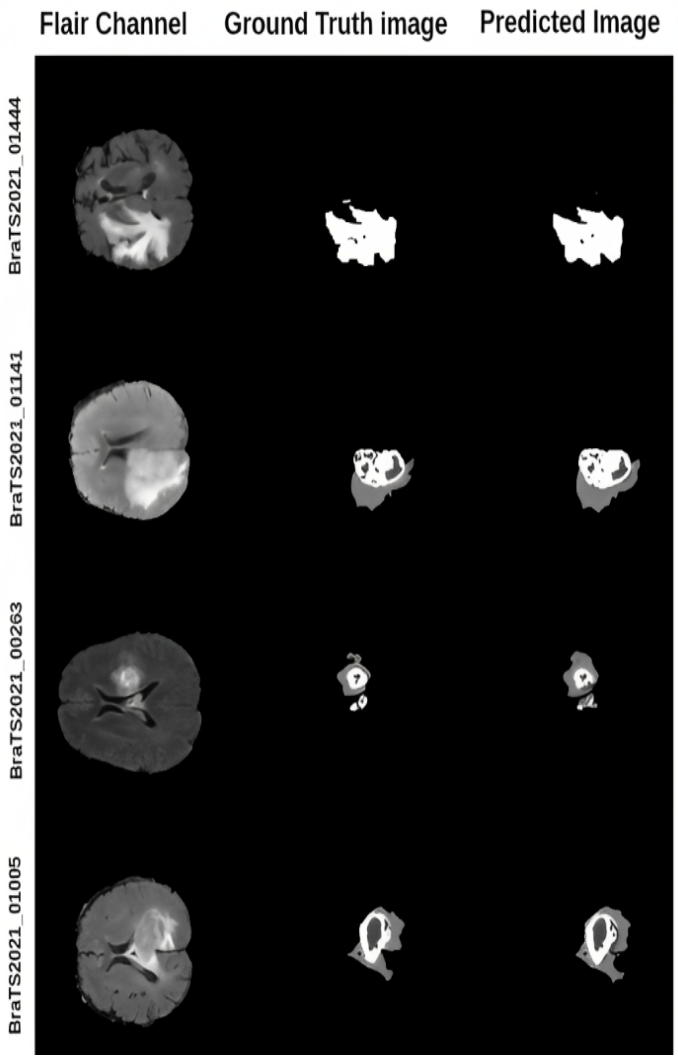

Fig. 11. Samples of segmentation results from the BraTS 2021 dataset.

TABLE IV. COMPARED SEGMENTATION RESULTS WITH DIFFERENT DSC METHODS FOR BRATS 2021

Author	Method	Whole	Core	Enhancing
Yan et al. [22]	U-Net	0.870	0.870	0.800
Ahmed et al. [23]	MS UNet	**0.919**	0.862	0.824
Raza et al. [24]	dResU-Net	0.866	0.835	0.800
Proposed	**Residual U-Net++**	0.903	**0.896**	**0.857**

TABLE V. MEAN SCORES OF TESTING DIFFERENT MODELS ON BRATS 2017, BRATS 2019, AND BRATS 2021 DATA FOR DSC, SENSITIVITY, SPECIFICITY, AND HAUSDORFF DISTANCE

Dataset	DSC	Sensitivity	Specificity	HD
BraTS 2017	0.876	0.94	**0.99**	11.2
BraTS 2019	0.892	0.96	**0.99**	10.2
BraTS 2021	**0.903**	**0.96**	**0.99**	**9.9**

V. DISCUSSION

The results show that the proposed Residual U-Net++ model uses three datasets: BraTS 2017, BraTS 2019, and BraTS 2021. We present the results for each dataset separately and evaluate it using four evaluation metrics: DSC, Sensitivity, Specificity, and HD.

Section IV-A shows the results for BraTS 2017. Table II, Regarding the DSC value of the whole tumor, core tumor, and enhancing tumor, Residual U-Net++ performs better than U-Net, ResU-Net, and AGResU-Net stand-alone approaches. Fig. 5 shows the box plot for the DSC results to observe that the almost results are above 80% from the first quartile and are at most 95%. To get a sense of them, its values representing HD are concluded in a box plot, as shown in Fig. 6.

Section IV-B shows the results for BraTS 2019. Table III, Regarding the DSC value of the whole tumor, core tumor, and enhancing tumor, Residual U-Net++ performs better than other approaches, especially ResU-Net as a stand-alone approach without nested U-Net. Fig. 7 shows the box plot for the DSC results to observe that the almost results are above 86% from the first quartile and are at most 94%. To get a sense of them, its values representing HD are concluded in a box plot, as shown in Fig. 8.

Section IV-C shows the results for BraTS 2021. Table IV, In terms of the DSC value of the core tumor and enhancing tumor, Residual U-Net++ performs better than other approaches. Also, it is slightly different from other top values of the whole tumor. Fig. 9 shows the box plot for the DSC results to observe that the almost results are above 87% from the first quartile and are at most 94%. To get a sense of them, its values representing HD are concluded in a box plot, as shown in Fig. 10.

From Table V, We get the complete results for all evaluation metrics: DSC, Sensitivity, Specificity, and HD, and for all datasets. We observe that BraTS 2021 gets more accurate results than BraTS 2019 and BraTS 2017, which is regarding the amount of data because BraTS 2021 is the largest dataset compared with BraTS 2019 and BraTS 2017. Also, BraTS 2019 gets more accurate results than BraTS 2017 for the same reason. Furthermore, the large amount of data gets more variant cases for the tumor.

This proposed model enhances the results compared with other approaches by 0.23 for the DSC value of the core tumor and 0.05 for the DSC value of the enhancing tumor. Fig. 11 shows samples of segmentation results for BraTS 2021.

VI. CONCLUSIONS

In this research, we proposed the Residual U-Net++ model, which combined ResU-Net modules and U-Net++ with a single U-Net design. Small-scale brain tumor segmentation was improved using ResU-Net++. We comprehensively evaluated the Residual U-Net++ model using three reliable BraTS 2017, BraTS 2019, and BraTS 2021 brain tumor standards. The results of the experiments demonstrated that Residual U-Net++ outperformed U-Net and ResU-Net. On all three datasets, the experimental results indicated that the suggested Residual U-Net++ model performed better in segmentation tasks when compared with other approaches, including UNet++ and other models. Due to the 2D U-Net model's limitations, Residual U-Net++ significantly lost local characteristics and context information across various slices. We will investigate 3D network design in the future to enhance Residual U-Net++ segmentation Net's performance and expand the enhanced architecture to other datasets to demonstrate its generalizability.

REFERENCES

[1] Nelly Gordillo, Eduard Montseny, and Pilar Sobrevilla. State of the art survey on mri brain tumor segmentation. *Magnetic resonance imaging*, 31(8):1426–1438, 2013.

[2] John SH Baxter, Eli Gibson, Roy Eagleson, and Terry M Peters. The semiotics of medical image segmentation. *Medical image analysis*, 44:54–71, 2018.

[3] Deepali Aneja and Tarun Kumar Rawat. Fuzzy clustering algorithms for effective medical image segmentation. *International Journal of Intelligent Systems and Applications*, 5(11):55–61, 2013.

[4] Jianxin Zhang, Zongkang Jiang, Jing Dong, Yaqing Hou, and Bin Liu. Attention gate resu-net for automatic mri brain tumor segmentation. *IEEE Access*, 8:58533–58545, 2020.

[5] Yu Weng, Tianbao Zhou, Yujie Li, and Xiaoyu Qiu. Nas-unet: Neural architecture search for medical image segmentation. *IEEE Access*, 7:44247–44257, 2019.

[6] Zan Li, Hong Zhang, Zhengzhen Li, and Zuyue Ren. Residual-attention unet++: A nested residual-attention u-net for medical image segmentation. *Applied Sciences*, 12(14), 2022.

[7] Haichun Li, Ao Li, and Minghui Wang. A novel end-to-end brain tumor segmentation method using improved fully convolutional networks. *Computers in biology and medicine*, 108:150–160, 2019.

[8] MD Nasim, Abdullah Al Munem, Maksuda Islam, Md Aminul Haque Palash, MD Haque, and Faisal Muhammad Shah. Brain tumor segmentation using enhanced u-net model with empirical analysis. *arXiv preprint arXiv:2210.13336*, 2022.

[9] Satyajit Maurya, Virendra Kumar Yadav, Sumeet Agarwal, and Anup Singh. Brain tumor segmentation in mpmri scans (brats-2021) using models based on u-net architecture. In *International MICCAI Brainlesion Workshop*, pages 312–323. Springer, 2022.

[10] Cheyu Hsu, Chunhao Chang, Tom Weiwu Chen, Hsinhan Tsai, Shihchieh Ma, and Weichung Wang. Brain tumor segmentation (brats) challenge short paper: Improving three-dimensional brain tumor segmentation using segresnet and hybrid boundary-dice loss. In *International MICCAI Brainlesion Workshop*, pages 334–344. Springer, 2022.

[11] MD Abdullah Al Nasim, Abdullah Al Munem, Maksuda Islam, Md Aminul Haque Palash, MD Mahim Anjum Haque, and Faisal Muhammad Shah. Brain tumor segmentation using enhanced u-net model with empirical analysis. *arXiv e-prints*, pages arXiv–2210, 2022.

[12] Ahliddin Shomirov, Jing Zhang, and Mohammad Masum Billah. Brain tumor segmentation of hgg and lgg mri images using wfl-based 3d u-net. *Journal of Biomedical Science and Engineering*, 15(10):241–260, 2022.

[13] Hengxin Liu, Guoqiang Huo, Qiang Li, Xin Guan, and Ming-Lang Tseng. Multiscale lightweight 3d segmentation algorithm with attention mechanism: Brain tumor image segmentation. *Expert Systems with Applications*, page 119166, 2022.

[14] Sachin Jain and Vishal Jain. Novel hybrid boosted ensemble learning framework for brain tumor prediction. In *2022 9th International Conference on Computing for Sustainable Global Development (INDIACom)*, pages 866–869. IEEE, 2022.

[15] Biswajit Jena, Sarthak Jain, Gopal Krishna Nayak, and Sanjay Saxena. Analysis of depth variation of u-net architecture for brain tumor segmentation. *Multimedia Tools and Applications*, pages 1–21, 2022.

[16] Carole H Sudre, Wenqi Li, Tom Vercauteren, Sebastien Ourselin, and M Jorge Cardoso. Generalised dice overlap as a deep learning loss function for highly unbalanced segmentations. In *Deep learning in medical image analysis and multimodal learning for clinical decision support*, pages 240–248. Springer, 2017.

[17] Adel Kermi, Issam Mahmoudi, and Mohamed Tarek Khadir. Deep convolutional neural networks using u-net for automatic brain tumor segmentation in multimodal mri volumes. In *International MICCAI Brainlesion Workshop*, pages 37–48. Springer, 2018.

[18] Lucas Fidon, Suprosanna Shit, Ivan Ezhov, Johannes C Paetzold, Sébastien Ourselin, and Tom Vercauteren. Generalized wasserstein dice loss, test-time augmentation, and transformers for the brats 2021 challenge. In *International MICCAI Brainlesion Workshop*, pages 187–196. Springer, 2022.

[19] Zia Khan, Norashikin Yahya, Khaled Alsaih, Mohammed Isam Al-Hiyali, and Fabrice Meriaudeau. Recent automatic segmentation algorithms of mri prostate regions: A review. *IEEE Access*, 2021.

[20] Nagwa M AboElenein, Songhao Piao, Alam Noor, and Pir Noman Ahmed. Mirau-net: An improved neural network based on u-net for gliomas segmentation. *Signal Processing: Image Communication*, 101:116553, 2022.

[21] Ning Sheng, Dongwei Liu, Jianxia Zhang, Chao Che, and Jianxin Zhang. Second-order resu-net for automatic mri brain tumor segmentation. *Mathematical Biosciences and Engineering*, 18(5):4943–4960, 2021.

[22] Benjamin B Yan, Yujia Wei, Jaidip Manikrao M Jagtap, Mana Moassefi, Diana V Vera Garcia, Yashbir Singh, Sanaz Vahdati, Shahriar Faghani, Bradley J Erickson, and Gian Marco Conte. Mri brain tumor segmentation using deep encoder-decoder convolutional neural networks. In *International MICCAI Brainlesion Workshop*, pages 80–89. Springer, 2022.

[23] Parvez Ahmad, Saqib Qamar, Linlin Shen, Syed Qasim Afser Rizvi, Aamir Ali, and Girija Chetty. Ms unet: Multi-scale 3d unet for brain tumor segmentation. In *International MICCAI Brainlesion Workshop*, pages 30–41. Springer, 2022.

[24] Rehan Raza, Usama Ijaz Bajwa, Yasar Mehmood, Muhammad Waqas Anwar, and M Hassan Jamal. dresu-net: 3d deep residual u-net based brain tumor segmentation from multimodal mri. *Biomedical Signal Processing and Control*, 79:103861, 2023.